

Signal Processing and Extensive Characterization Method of Heart Sounds Based on Wavelet Analysis

R. Hendradi¹, A. Arifin^{1,5}, H. Shida², S. Gunawan³, M. H. Purnomo¹,
H. Hasegawa⁴, H. Kanai²

Abstract – One of the valuable methods of cardiac valve diagnosis can be performed by auscultation. We proposed a signal processing and extensive characterization method based on wavelet analysis to investigate important characteristics of heart sounds of normal and pathologic systolic murmur human subjects. Time-scale maps yielded by wavelet transform calculation were solved using magnitude thresholding operation and centre of gravity to restrict temporal and frequency-related of valvular activities. From our experimental results, temporal and frequency-related parameters of S_1 , S_2 , and their components could be characterized precisely. Application of our method was adequate to characterize the heart sounds objectively, clearly, systematically, and comprehensively. The method was considered valuable to explain mechanisms of cardiac valves functions. We expected that the method would be helpful for clinical diagnosis as well as developing of heart sound modelling and educational purpose. Next topic of our study was addressed for classification of the heart sounds. **Copyright © 2016 Praise Worthy Prize S.r.l. - All rights reserved.**

Keywords: Centre of Gravity, Heart Sound, Thresholding Method, Wavelet Transform

Nomenclature

A_2	Aortic component
$C(b,a)$	Wavelet coefficients of time location b and scale factor a
c_{con}	Thresholding coefficient of contour
c_{env}	Thresholding coefficient of the Shannon envelope
$E_x(t)$	Average Shannon energy for frame t
g	Mother wavelet
m_{max}	Maximum of the normalized magnitude
m_{min}	Minimum of the normalized magnitude
M_1	Mitral component
$M(E_x(t))$	Mean of average Shannon energy for frame t
p_{max}	Maxima of Shannon envelope in segmentation with respect to a cardiac cycle
p_{min}	Minima of Shannon envelope in segmentation with respect to a cardiac cycle
P_2	Pulmonic component
$P(t)$	Shannon envelope for frame t
s_{COG}	Scale-coordinate of Centre of Gravity
s_h	Higher scale
s_l	Lower scale
s_{rg}	Frequency range in scale
S_1	First heart sound
S_2	Second heart sound
t_{COG}	Time-coordinate of Centre of Gravity
t_{dur}	Duration in s
t_h	Higher time
t_l	Lower time
T_1	Tricuspid component

$S(E_x(t))$	Standard deviation of average Shannon energy for frame t
$x(i)$	i^{th} original heart sound signal
$x_{norm}(i)$	i^{th} normalized signal of heart sound

I. Introduction

Heart disease is the second most lethal disease after cerebrovascular accident [1]. An early, non-invasive detection of the heart diseases, with particular procedures and follow-up treatments can prevent increasing of fatal risks of the heart attacks [2]-[5]. One of the procedures for early detection of heart disease can be conducted through diagnosis of heart sounds [1], [6].

Heart sounds are the sounds yielded by some mechanical activities of the heart during a cardiac cycle.

The factors that may be connected with the production of the heart sounds, i.e., cardiac muscles contraction, movements of the cardiac valves, movements of cardiac wall, and flows of the blood through the chambers and blood vessels of the heart. The cardiac cycle has two phases: systole and diastole. During systole, an active full contraction of ventricles that forces blood out from the heart; during diastole, a relaxation of the ventricles and the heart is filled with blood. A normal functioning heart comprises of two basic heart sounds: S_1 as a first heart sound and S_2 as a second heart sound [7].

Generation of S_1 sound coincides with contraction of the ventricles, thus identifying the onset of ventricular systole and the end of mechanical diastole.

The S_1 sound is produced of compound in nature by three stages [8], [9]: firstly, low-frequency beginning, due to myocardial tension. Secondly, higher-frequency central stage, due to valvular events; the central stage contains at least four vibrations that correlate with the motion of the four valves in the following order: mitral (M_1) closing, tricuspid (T_1) closing, pulmonic (P_2) opening, and aortic (A_2) opening.

Only the first two are normally audible. Thirdly, low-frequency final stage, due to vascular phenomena that produced by rapid ejection of blood. The vibrations of the S_2 identify the onset of ventricular diastole and occur at the end of mechanical systole.

The S_2 sound is generated of three stages as well as the S_1 sound [8], [9]: firstly, low-frequency beginning, due to eddies preceding the valvular closure. Secondly, central stage of higher-frequency, due to closing of the semilunar valves (A_2 and P_2). Thirdly, final stage of low-frequency, because of final vibrations and opening of the atrioventricular valves (T_1 and M_1).

If opening of heart valve is not perfect or stenosis which force blood through a narrow opening, or regurgitation caused by valve closure is not perfect and resulted in backflow of blood, then will be resulted additional sound. An Abnormal heart sound arises as a result of turbulence flow of blood that passes through narrow openings is called murmur [7].

One of the valuable methods of cardiac valve diagnosis can be performed by auscultation [1], [6].

The auscultation is a traditional technique in clinical diagnosis that is performed by listening to the heart sounds using a stethoscope. The heart sounds analysis by auscultation technique is a difficult skill. Accurateness of the analysis relies greatly on the expertise and practical knowledge of a listener that takes years to acquire and refine [10]. Because this skill is highly tough to be taught in a structured way, so that hearing of a cardiologist with another one who cannot be copied, although this technique has been studied both in educational and clinical aspects in medicine through standard literatures [7], [11], [12]. Therefore, the above problems and subjectivity of a cardiologist become deteriorations of auscultation technique.

Limitations of traditional auscultation have motivated us to develop a signal processing method that explored essential characteristics of the heart sounds. In previous research, Fast Fourier Transform (FFT) presented valuable frequency information about M_1 and T_1 (the S_1 components) also A_2 and P_2 (the S_2 components) of a normal heart sound [13]. Nevertheless, the FFT did not allocate frequency content evidence localized in time, so it could not reveal which of two valves were closed firstly. Moreover, Lee et al. [14] have investigated the exact features of heart sound using Short Time Fourier Transform (STFT). However, STFT could not perceive M_1 and T_1 also imprecisely identified A_2 and P_2 .

This problem was caused by selection of length of a time window and a trade-off between time and frequency resolutions.

Debbal and Bereksi-Reguig [13], [15] and Vikhe et al. [16] analysed the A_2 - P_2 split using Wavelet Transform method. However, the method did not clearly explain how to measure their split time. Furthermore, there were lack of measuring data only at adjacent condition in time of their time-scale maps of A_2 and P_2 , whereas both time-scale maps could also be appeared as a single component and overlapping conditions.

We proposed a signal processing and extensive characterization method based on wavelet analysis to investigate essential characteristics of the heart sounds of normal and pathologic systolic murmur human subjects.

Time-scale maps yielded by wavelet transform calculation were solved using magnitude thresholding operation and Centre of Gravity (COG) to restrict temporal and frequency-related evidence of valvular activities.

The temporal and frequency-related parameters are duration of S_1 and S_2 , S_1 - S_2 spaced time, events of M_1 and T_1 during systole, A_2 and P_2 during diastole, and physiological split time between valve events in each cardiac sub-cycle. The COG of each thresholding wavelet transform contour was used to acquire appropriately the S_1 - S_2 spaced time, the M_1 - T_1 split, the A_2 - P_2 split, respectively. Hence, characteristics of each pattern of the heart sounds can be extracted more precisely. The proposed method would be useful for diagnosis and for understanding about mechanisms of cardiac valves function. Moreover, the method promises an important role in development of heart sound modelling and study of auscultation technique for medical students.

II. Methods

II.1. Data Collection

The heart sound recordings were consisted of two parts. One was collected from an acoustic transducer of ALOKA ProSound II SSD-6500 SV and the recordings were digitized with 1 kHz sampling frequency.

The other was from 3M Littmann Model 4100 electronic stethoscope and the recordings were digitized with 8 kHz sampling frequency.

Two subjects (men, age: 23 and 39 years, body height: 172 and 170 cm, body weight: 57 and 76 kg) without a murmur (normal) and two other subjects (man and woman, age: 54 and 54 years, body height: 160 and 160 cm, body weight: 63 and 67 kg) of pathologic systolic murmur, i.e., mitral valve regurgitation (MR) and tricuspid valve regurgitation (TR), respectively, were participated in this study. Purpose of an experiment was explained to each subject and subject's consent was obtained.

The heart sound recording was performed at four different auscultation areas, i.e. mitral, tricuspid, aortic, and pulmonary areas for both normal subjects to acquire best sounds. Moreover, both murmur subjects were achieved at mitral area for MR subject and tricuspid area for TR subject by a cardiologist.

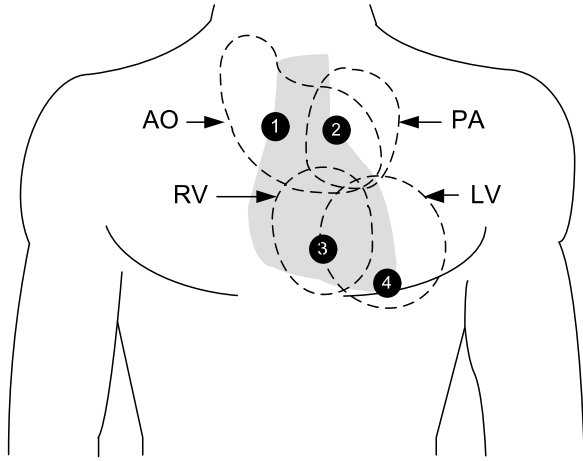


Fig. 1. Auscultation sites. AO = aortic area; PA = pulmonic area; RV = right ventricle area; LV = left ventricle area; 1 = right second intercostal space; 2 = left second intercostal space; 3 = mid-left sternal border (tricuspid area); 4 = fifth intercostal space, midclavicular line (mitral area)

The aortic area sited in the second intercostal space along the right sternal border, as shown in Fig. 1.

The pulmonic area sited in the second intercostal space at the left sternal border. The tricuspid area located in the fifth intercostal space along the left sternal border.

The mitral area sited in the fifth intercostal space near the midclavicular line. The recording was conducted in two different conditions, inspiratory and expiratory apnea, to reduce noise from breathing [17].

The recording was obtained in a quiet recording environment from the sitting upright subject (for the normal subjects) and from the supine subject on a bed (for the murmur subjects).

II.2. Signal Processing

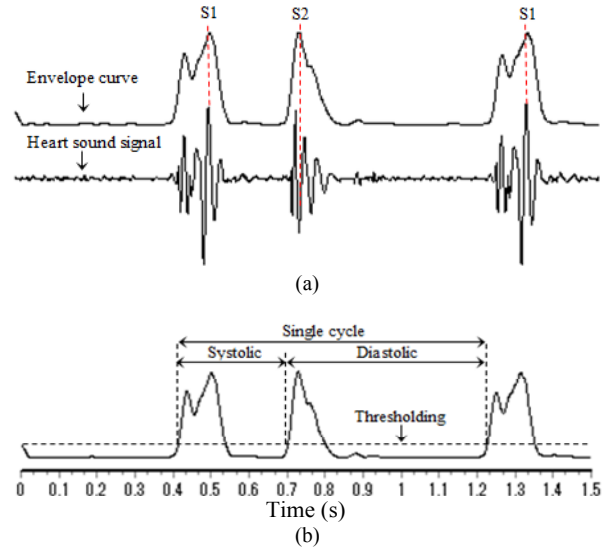
Signal processing of the heart sounds consisted of three steps as follows: pre-processing for filtering, segmentation with respect to the cardiac cycle, and feature extraction to restrict temporal and frequency-related of valvular events. In this study, the signal processing method was performed using Pascal programming language.

II.3. Pre-processing

Two phases filtering to decrease interference caused by background noise were performed. Firstly, a bandpass IIR filter of eighth-order Butterworth with cut-off 20 Hz and 330 Hz was used from an original signal.

The original signal of 8 kHz sampling frequency was decimated by factor 4 to 2 kHz. Picking of bandwidth adequate with [12]. Furthermore, segmentation of the signal based on envelope curve that would be explained later. Secondly, algorithm of wavelet denoising of the fixed threshold depicted in Hall et al. [18] was implemented for enhancing quality of the signal.

A Daubechies wavelet of order 4 (Db4) with fifth decomposition level was selected.



Figs. 2. Illustration of mechanism of segmentation. (a) Envelope curve and heart sound signal. (b) Definition of systolic, diastolic, and single cycle from its envelope curve

II.4. Segmentation

Segmentation with respect to the cardiac cycle was an important step in analysing of the heart sounds. Detection the location and intervals of S_1 and S_2 could be very helpful information about the condition of the mechanical activity of the heart. Mechanism of segmentation is described on Figs. 2 using normalized average Shannon energy. The original signal would be expressed in more simply and easily seen by utilizing of the envelope curve based on the S_1 and the S_2 (Fig. 2(a)).

Shannon envelope, i.e., the normalized average Shannon energy is the popular envelope technique.

The method was capable to attenuate the effect of low value noise and to make the low intensity sounds easier to be found [19]. The algorithm was depicted in following. Firstly, an original heart sound was normalized by absolute maximum of the signal, $\max|x(\cdot)|$, as in Eq. (1):

$$x_{norm}(i) = \frac{x(i)}{\max(|x(\cdot)|)} \quad (1)$$

Secondly, the average Shannon energy was calculated using Eq. (2):

$$E_x = -\frac{1}{N} \sum_{i=1}^N x_{norm}^2(i) \cdot \log x_{norm}^2(i) \quad (2)$$

where $x_{norm}(i)$ was the i^{th} normalized signal and N was the number of points in 0.02 s segment (normal subject) and 0.0165 s segment (murmur subject), which corresponds to a frame, here $N = 20$ (normal subject) and $N = 33$ (murmur subject). Thirdly, the average Shannon energy was normalized over all of the frames, so the Shannon envelope became Eq. (3):

$$P(t) = \frac{E_x(t) - M(E_x(t))}{S(E_x(t))} \quad (3)$$

where $E_x(t)$ was the average Shannon energy for frame t , $M(E_x(t))$ was the mean of $E_x(t)$, and $S(E_x(t))$ was the standard deviation of $E_x(t)$ [19]. Fourthly, the Shannon envelope was then filtered reverse direction.

The resulting sequence had precisely zero phase filter, so there was no time delay.

The amplitude peaks of S_1 , S_2 , and S_1 of the next cycle of Shannon envelope were identified that based on visual inspection. Basic knowledge of the S_1 and S_2 peaks identification that the diastole is longer than the systole [11]. The peak adjacent to the longest interval (diastolic) was identified as S_2 . Furthermore, the peak adjacent to the shortest interval (systolic) was identified as S_1 [19]. Maximum among the three peaks, namely p_{max} , was obtained. Then, minimum, p_{min} , of interval that contained the three peaks was acquired. Furthermore, the thresholding (horizontal dotted line on Fig. 2(b)) was done equal to $p_{min} + c_{env} \times p_{max}$, where c_{env} was a thresholding coefficient of the Shannon envelope. Selection of c_{env} was set manually and varied ($0.01 < c_{env} < 0.50$). Its selection based on onset until ending events of S_1 and S_2 , respectively, also beginning of S_1 of the next cycle as shown in Fig. 2(b). The single cycle is time interval between beginning of S_1 of a cycle and beginning of S_1 of the next cycle. The systolic is time interval between beginning of S_1 until beginning of S_2 .

The diastolic is time interval between beginning of S_2 until beginning of S_1 of the next cycle (Fig. 2(b)).

II.5. Feature Extraction

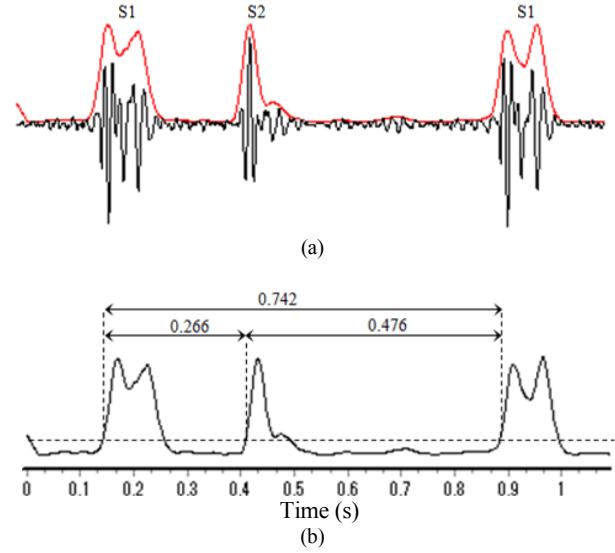
A feature extractor, i.e., Continuous wavelet transform (CWT) is suitable for the analysis of non-stationary heart sound signals. CWT uses a variable sized window region. Because the wavelet may be compressed or dilated, different features of the signal are extracted.

While a stretched wavelet picks up on the lower frequency components, a narrow wavelet extracts high-frequency components. The method is a multiresolution analysis that can simultaneously represent time and frequency information of the signals by using a flexible window modulation. Hence, characteristics of each pattern of the signals can be extracted more precisely.

Computation of CWT was related to the signal $x(t)$ with families of time frequency atoms $g(t)$; it formed a set of coefficients $C(b,a)$ specified in Eq. (4):

$$C(b,a) = \frac{1}{\sqrt{a}} \int_{-\infty}^{\infty} x(t) g^* \left(\frac{t-b}{a} \right) dt \quad (4)$$

where b was the time location, a was the scale factor and it was inversely proportional to the frequency ($a > 0$), symbol * represents a complex conjugate, and $g(t)$ was the mother wavelet.



Figs. 3. An example of segmenting signal. (a) A filtered normal signal and its Shannon envelope. (b) The values for single cycle, systolic, and diastolic of the envelope curve

Function $g(t)$ should fulfil the most crucial properties, i.e., continuity, integrability, square integrability, progressivity and that it has no d.c. component [20].

Additionally, the mother wavelet $g(t)$ has to be concentrated in both time and frequency as much as possible. It is acknowledged that the smallest time bandwidth product is attained by the Gaussian function [21]. As pointed out of [22], Morlet wavelet was a complex exponential modulated Gaussian function of the form Eq. (5):

$$g(t) = e^{-i\omega_0 t} e^{-\frac{t^2}{2}} \quad (5)$$

where $\omega_0 = \pi \sqrt{\frac{2}{\ln 2}} = 5.336 \text{ rad/s}$ ($f_0 = 0.849 \text{ Hz}$).

The most reliable wavelet for the time-frequency of heart sound signals is the Morlet wavelet [23].

The wavelet coefficients C , in the matrix form, were function of both b and a (Eq. (4)). The wavelet coefficients C , in colour spectrum, were depicted as normalized magnitude [0,1], where the lowest and the highest intensity correspond to purple and red, respectively. The pattern was 200×100 (time \times scale) with scale factors 1.0×10^{-2} up to 1.0×10^{-1} . In this research, an extensive characterization method based on wavelet analysis consisted of magnitude thresholding operation and Centre of Gravity (COG). The magnitude thresholding operation was conducted to acquire time-scale parameters that correspond to characterization of the heart sounds. When the normalized magnitude value greater than or equal to a predetermined value, one or more thresholding contours would be obtained. The thresholding was done equal to $m_{min} + c_{con} \times m_{max}$, where m_{min} was minimum of the normalized magnitude, c_{con} was thresholding coefficient of contour, and m_{max} was maximum of the normalized magnitude.

Selection of c_{con} was set manually and varied ($0.01 < c_{con} < 0.99$). Its selection depended on onset until ending event as well as lowest to highest scale. The time-scale maps of the thresholding method gave more simply and easily seen. Therefore, low of contour time (t_l), high of contour time (t_h), contour duration (t_{dur}), low of contour scale (s_l), high of contour scale (s_h), and contour scale range (s_{rg}) could be obtained.

These parameters were associated with duration ($t_{dur} = t_h - t_l$) and frequency range ($s_{rg} = s_h - s_l$) of S_1 , S_2 , S_1 and S_2 components, respectively. Furthermore, COG is a pivotal point that associated with the thresholding contour. If COG coordinate of a collection of wavelet coefficients was (t_{COG} , s_{COG}), time-coordinate of COG, t_{COG} , was abscissa and scale-coordinate of COG, s_{COG} , was ordinate. The t_{COG} of each thresholding contour of S_1 , S_2 , S_1 and S_2 components, was utilized to acquire the S_1 - S_2 spaced time, the M_1 - T_1 split, the A_2 - P_2 split, respectively.

The S_1 - S_2 spaced time was difference between t_{COG} of S_1 and t_{COG} of S_2 . The M_1 - T_1 split was difference between t_{COG} of M_1 and t_{COG} of T_1 . The A_2 - P_2 split was difference between t_{COG} of A_2 and t_{COG} of P_2 .

II.6. Statistical Analysis

Results of the experimental data were expressed as mean \pm SD. Student's t-test (significance level: 0.001) for normal distribution variables was used to compare difference data between inspiratory apnea and expiratory apnea groups in time domain and frequency domain (in scale). For each single cycle, S_1 , and S_2 , hypothetical test was calculated based on the duration and the range scale of each group. Whereas, M_1 and T_1 also A_2 and P_2 were calculated based on t_{COG} and s_{COG} , respectively.

III. Results

Three groups of subjects: normal, MR and TR, were segmented. From the segmentation algorithm based on Shannon envelope, 137 signals of the normal, 9 signals of the MR and 22 signals of the TR for single cycle, systole, and diastole were obtained, respectively. Figs. 3 depict an example of segmenting signal that relates to the cardiac cycle using Shannon envelope of the normal subject. Table I shows t_{dur} of diastolic is longer than systolic for the three groups. In this study, exploration of important characteristics of the heart sounds, each single cycle that contained both systole and diastole were extracted by utilizing extensive characterization method based on wavelet analysis. Figs. 4, Figs. 6, and Figs. 7 show example of normal, MR, and TR subjects, respectively. These figures have S_1 and S_2 components at overlapping conditions. Figs. 5 depict S_1 components at adjacent condition (Fig. 5(a)) and S_2 appears like a single component condition (Fig. 5(d)).

In our experimental results, from these time-scale maps, the temporal and frequency-related parameters could be localized. Table I shows that t_{dur} of S_1 , in systole, is longer than S_2 , in diastole for the three groups

of subjects. Moreover, the S_1 - S_2 spaced time of the normal subject is less than the murmur subject. Additionally, S_1 has wider s_{rg} and higher s_h than S_2 for the three groups.

Two basic components of the S_1 sound are the M_1 component and the T_1 component. In this study, we have acquired 81, 4, and 2 systoles that contained M_1 and T_1 from normal, MR, and TR data, respectively. Fig. 4(c) shows an example of the normal subject that t_{dur} of M_1 is 0.0347 sec., where t_l is 0.0120 sec. (localized at 4.5% of systole position) and t_h is 0.0467 s (localized at 17.5% of systole position). Similarly, all calculations of t_{dur} of M_1 are shown in Table I. Fig. 4(c) also shows that t_{dur} of T_1 is 0.0788 s., where t_l is 0.0254 s (localized at 9.5% of systole position) and t_h is 0.1041 s (localized at 39.0% of systole position).

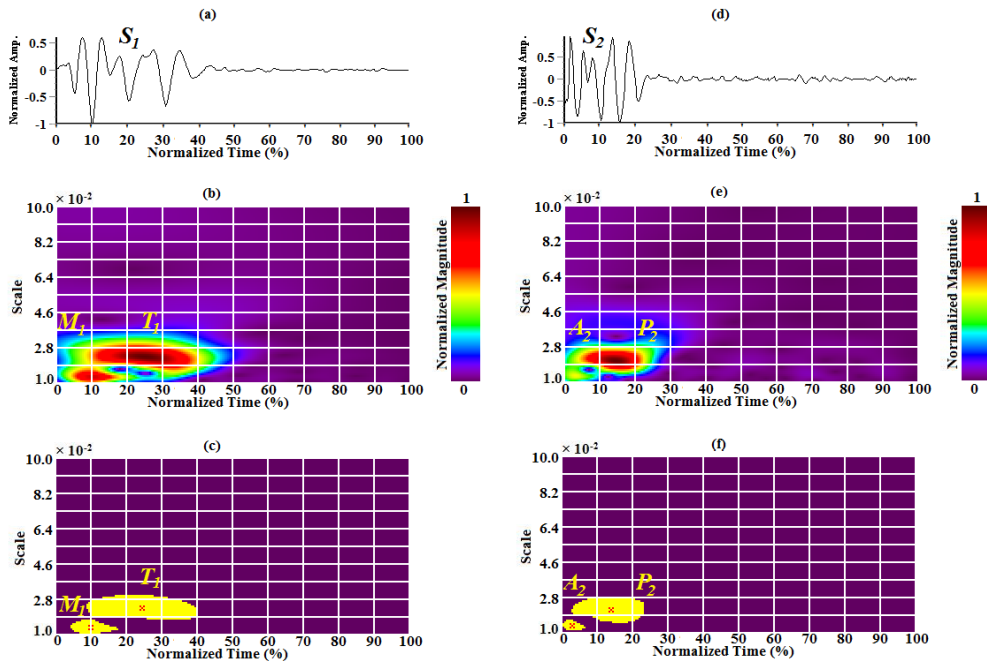
All similar calculations of t_{dur} of T_1 are shown in Table I. Furthermore, T_1 has longer t_{dur} than M_1 for the normal and MR except the TR subject. Moreover, M_1 and T_1 valves close at the beginning of ventricular systole. The M_1 valve usually closes slightly before the T_1 valve (e.g. Fig. 4(b)). Thus, both components of S_1 can be distinguished separately by time delay. The time delay referred as physiological split time [9] or normal split time. The time delay between them plays very vital role in medical diagnosis. Fig. 4(c) shows that the M_1 - T_1 split is 0.0387 s, where t_{COG} of M_1 is 0.0267 s (localized at 10.0% of systole position) and t_{COG} of T_1 is 0.0654 s (localized at 24.5% of systole position) (in red crosses).

The similar result is shown in Table I for the three groups of subjects. Furthermore, Fig. 4(c) shows that s_{rg} of the thresholding M_1 contour is 0.0070, where s_l is 0.0110 and s_h is 0.0180. Whereas, s_{rg} of the thresholding T_1 contour is 0.0130, where s_l is 0.0190 and s_h is 0.0320. Table I shows the similar result that T_1 has wider s_{rg} and higher s_h than M_1 for the three groups.

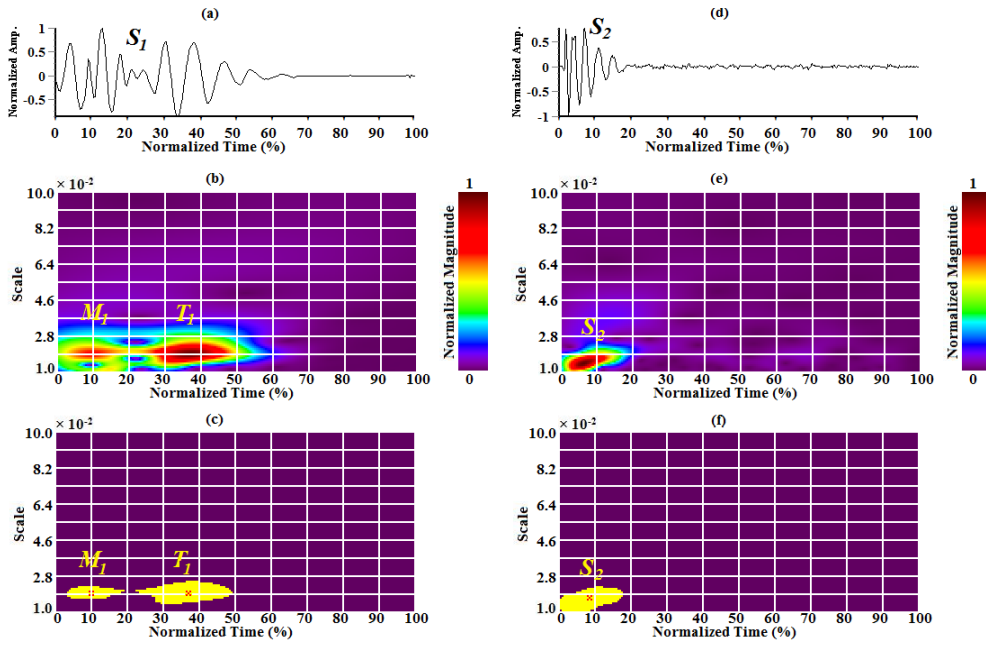
Two basic components of the S_2 sound are the A_2 component and the P_2 component. Both of these valves close at the end of ventricular systole. Normally, the A_2 valve closes slightly ahead of the P_2 valve because closing pressure is higher in the aorta than in the pulmonary artery. Therefore, A_2 usually occurs earlier and is louder than P_2 (e.g. Fig. 4(e)), contrarily in some pathological cases A_2 and P_2 may be reversed in time order [7]. From the experimental data, we have acquired 15, 2, and 7 diastoles that contained A_2 and P_2 from normal, MR, and TR data, respectively. Fig. 4(e) shows an example of the normal subject that t_{dur} of A_2 is 0.0259 s, where t_l is 0.0022 s (localized at 0.5% of diastole position) and t_h is 0.0281 s (localized at 6.5% of diastole position). Similarly, all calculations of t_{dur} of A_2 are shown in Table I. Fig. 4(e) also shows that t_{dur} of P_2 is 0.0864 s, where t_l is 0.0130 s (localized at 3.0% of diastole position) and t_h is 0.0994 s (localized at 23.0% of diastole position). All similar calculations of t_{dur} of P_2 are shown in Table I. Table I shows that t_{dur} of P_2 is longer than A_2 except for MR subject. Fig. 4(f) shows that s_{rg} of the thresholding A_2 contour is 0.0050, where s_l is 0.0120 and s_h is 0.0170.

TABLE I
TEMPORAL AND SCALE PARAMETERS OF THE NORMAL, THE MR, AND THE TR SUBJECTS, RESPECTIVELY

Parameter	Conditions of Normal		Conditions of MR		Conditions of TR		
	Inspiratory apnea	Expiratory apnea	Inspiratory Napnea	Expiratory apnea	Inspiratory apnea	Expiratory apnea	
t_{dur} of single cycle (s)	0.749±0.089	0.782±0.066	0.869±0.053	0.857±0.072	0.782±0.029	0.745±0.021	
t_{dur} of systolic (s)	0.275±0.027	0.277±0.021	0.311±0.015	0.326±0.022	0.311±0.012	0.323±0.012	
t_{dur} of diastolic (s)	0.475±0.072	0.505±0.055	0.559±0.042	0.531±0.058	0.471±0.022	0.422±0.015	
S_1	t_{dur} (s)	0.123±0.033	0.125±0.030	0.141±0.017	0.176±0.049	0.137±0.026	0.126±0.013
	S_l	0.013±0.002	0.012±0.002	0.020±0.004	0.034±0.010	0.019±0.003	0.018±0.002
	S_h	0.037±0.007	0.037±0.007	0.050±0.002	0.068±0.003	0.065±0.013	0.057±0.006
	S_{rg}	0.024±0.009	0.025±0.007	0.030±0.004	0.034±0.013	0.046±0.015	0.040±0.006
S_2	t_{dur} (s)	0.096±0.020	0.091±0.018	0.118±0.021	0.137±0.022	0.095±0.017	0.095±0.015
	S_l	0.012±0.001	0.012±0.002	0.025±0.007	0.023±0.001	0.026±0.003	0.026±0.007
	S_h	0.034±0.005	0.033±0.005	0.048±0.004	0.060±0.003	0.048±0.006	0.044±0.006
	S_{rg}	0.022±0.005	0.021±0.005	0.023±0.011	0.037±0.003	0.023±0.005	0.018±0.004
M_1	t_{dur} (s)	0.045±0.023	0.037±0.026	-	0.046±0.009	0.134±0.003	-
	S_l	0.015±0.002	0.013±0.002	-	0.028±0.002	0.023±0.000	-
	S_h	0.024±0.005	0.021±0.003	-	0.042±0.005	0.043±0.001	-
	S_{rg}	0.009±0.004	0.009±0.004	-	0.013±0.003	0.020±0.001	-
T_1	t_{dur} (s)	0.054±0.029	0.065±0.035	-	0.115±0.006	0.118±0.047	-
	S_l	0.018±0.006	0.019±0.004	-	0.044±0.006	0.053±0.001	-
	S_h	0.029±0.010	0.031±0.006	-	0.066±0.003	0.067±0.004	-
	S_{rg}	0.011±0.007	0.013±0.008	-	0.021±0.009	0.014±0.005	-
A_2	t_{dur} (s)	0.035±0.021	0.013±0.002	0.074±0.050	-	0.062±0.031	0.041±0.051
	S_l	0.012±0.001	0.014±0.001	0.023±0.003	-	0.024±0.003	0.017±0.003
	S_h	0.020±0.006	0.020±0.002	0.042±0.008	-	0.041±0.006	0.027±0.012
	S_{rg}	0.007±0.006	0.005±0.002	0.019±0.005	-	0.017±0.008	0.010±0.011
P_2	t_{dur} (s)	0.071±0.016	0.068±0.016	0.038±0.026	-	0.040±0.004	0.085±0.020
	S_l	0.020±0.006	0.024±0.002	0.032±0.008	-	0.059±0.009	0.035±0.019
	S_h	0.033±0.005	0.033±0.002	0.040±0.016	-	0.074±0.005	0.051±0.018
	S_{rg}	0.012±0.003	0.009±0.004	0.008±0.007	-	0.015±0.004	0.016±0.003
t_{COG} of S_1 (s)	0.064±0.011	0.061±0.012	0.062±0.008	0.111±0.019	0.062±0.015	0.054±0.007	
t_{COG} of S_2 (s)	0.315±0.028	0.318±0.031	0.350±0.023	0.374±0.016	0.338±0.016	0.356±0.022	
S_1 - S_2 spaced time (s)	0.251±0.029	0.257±0.024	0.287±0.021	0.264±0.010	0.276±0.015	0.302±0.021	
t_{COG} of M_1 (s)	0.038±0.011	0.030±0.013	-	0.031±0.008	0.068±0.001	-	
t_{COG} of T_1 (s)	0.072±0.016	0.068±0.014	-	0.128±0.034	0.105±0.012	-	
M_1 - T_1 split (s)	0.034±0.017	0.040±0.016	-	0.096±0.027	0.037±0.011	-	
t_{COG} of A_2 (s)	0.021±0.006	0.016±0.006	0.039±0.012	-	0.026±0.013	0.011±0.003	
t_{COG} of P_2 (s)	0.055±0.013	0.068±0.001	0.087±0.031	-	0.024±0.006	0.056±0.018	
A_2 - P_2 split (s)	0.034±0.013	0.052±0.006	0.049±0.018	-	0.011±0.004	0.045±0.015	



Figs. 4. An example of S_1 and S_2 components at overlapping condition (in time) of the normal subject. (a) Example of well separated M_1 and T_1 . (b) Wavelet coefficients of (a) in colour spectrum. The colour spectrum is normalized magnitude of wavelet coefficient [0, 1], where the lowest and the highest intensity correspond to purple and red, respectively. (c) The thresholding M_1 and T_1 contours of (b) and their COG coordinates (red crosses). (d) Example of well separated A_2 and P_2 . (e) Wavelet coefficients of (d). A format similar to that of Fig. 4(b) (f) The thresholding A_2 and P_2 contours of (e) and their COG coordinates (red crosses)

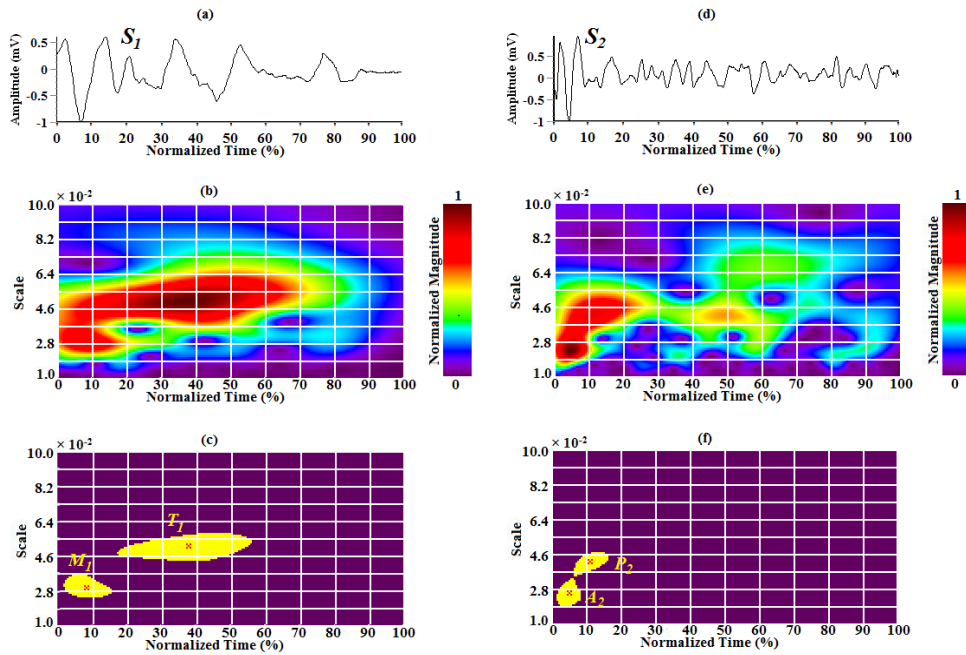


Figs. 5. An example of S_1 components at adjacent condition and S_2 appears like a single component (in time) of the normal subject. (a) Example of separated M_1 and T_1 . (b) and (e) are wavelet coefficients for (a) and (d), respectively. A format similar to that of Figs. 4 is used. (c) The thresholding M_1 and T_1 contours of (b) and their COG coordinates (red crosses). (d) S_2 appears like a single component. (f) The thresholding S_2 contour of (e) and its COG coordinate (red cross)

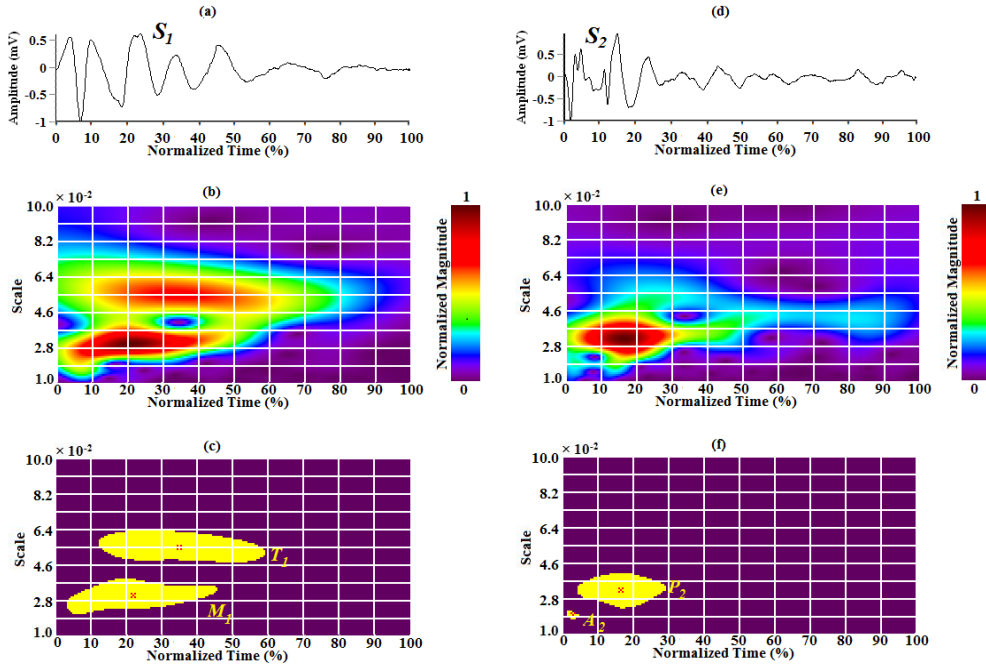
Whereas, s_{rg} of the thresholding P_2 contour is 0.0130, where its s_l is 0.0160 and s_h is 0.0290.

Table I shows the similar result that P_2 has wider s_{rg} and higher s_h than A_2 for normal and TR except MR subject. For significance level 0.001 by paired sample t-test that there was no statistically significance difference between inspiratory apnea group and expiratory apnea group of each time-scale parameter, i.e. single cycle

(except for the normal subject in t_{dur}), S_1 , S_2 , also M_1 , T_1 , A_2 , and P_2 components (except for MR and TR subjects, respectively, because each subject has no paired sample group). For the time parameter of single cycle, there was t_{dur} of its expiratory apnea longer than its inspiratory apnea. This indicates that the recording can be conducted on expiratory apnea or inspiratory apnea condition.



Figs. 6. An example of S_1 and S_2 components at overlapping condition (in time) of the MR subject. (a) and (d) are example of well separated M_1 and T_1 , A_2 and P_2 , respectively. (b) and (e) are wavelet coefficients for (a) and (d), respectively. A format similar to that of Figs. 4 is used. (c) The thresholding M_1 and T_1 contours of (b) and their COG coordinates (red crosses). (f) The thresholding A_2 and P_2 contours of (e) and their COG coordinates (red crosses)



Figs. 7. An example of S_1 and S_2 components at overlapping condition (in time) of the TR subject. (a) and (d) are example of well separated M_1 and T_1 , A_2 and P_2 , respectively. (b) and (e) are wavelet coefficients for (a) and (d), respectively. A format similar to that of Figs. 4 is used. (c) The thresholding M_1 and T_1 contours of (b) and their COG coordinates (red crosses). (f) The thresholding A_2 and P_2 contours of (e) and their COG coordinates (red crosses)

IV. Discussions

In early part of the experiment of this study, all recording data were inspected and explained in Methods Section. The heart sound recordings from all subjects apparently did not have different characteristics for obtaining S_1 , S_2 , and their components in relation to the auscultation locations. Furthermore, no statistically significance different (significance level: 0.001) of all subjects between inspiratory apnea group and expiratory apnea group for t_{dur} of S_1 and S_2 , S_1 - S_2 spaced time, t_{dur} of M_1 and T_1 , M_1 - T_1 split, t_{dur} of A_2 and P_2 , and A_2 - P_2 split. Also for s_{rg} of S_1 and S_2 , and s_{COG} of component M_1 , T_1 , A_2 , and P_2 , respectively. Additionally, the auscultation site of pulmonic area in capturing A_2 and P_2 components of all subjects at both inspiratory apnea and expiratory apnea conditions could not be obtained.

The split S_2 may be absent because it is influenced by the amount of tissue between the source of the sound and outer chest wall. Fat, muscle, and air tend to reduce sound transmission [7]. Moreover, sensitivity of the acoustic transducer also affected the recordings. Hence the placement of the acoustic transducer could not be specified in one point. Thus, the same statistical analysis to capture characteristics of the heart sounds was applied.

The segmentation with respect to the cardiac cycle was an important step in analysing of the heart sounds. Picking the thresholding (horizontal dotted line on Fig. 3(b)) would truncate heart sound signal at certain points to obtain the onset until the ending events of S_1 and S_2 , respectively, also beginning of S_1 of the next cycle. Its thresholding depended on c_{env} value. Variation of c_{env} of the normal and pathologic systolic murmur (MR and TR)

subjects strongly depended on the measurement condition and individual variation. Therefore, we were set its c_{env} to have a proper thresholding for consistent outcomes manually.

In our experimental results, the abnormal recordings were very complicated and the patterns vary largely from recording to recording. Two of four times the recording on the MR subject were neglected. The sudden release for a short time during the recording of the stethoscope from the subject had resulted in incorrect detection. Furthermore, the problems for picking up the peaks, i.e., many extra peaks and artefact that as though real peaks both in amplitude and time interval. Large intensity murmur overlapped with S_1 or S_2 would make the proper identification and segmentation improbable.

The heart sounds are non-stationary and complex signals. Therefore, thresholding operation of wavelet coefficients should be performed to obtain temporal and frequency-related parameters that associated with their characterizations. The time-scale maps of the thresholding method gave more simply and easily seen. Picking the thresholding value depended on c_{con} value. Variation of c_{con} of the subject highly depended on the measurement condition and individual variation such as variation c_{env} in segmentation with respect to the cardiac cycle. Therefore, we were set its c_{con} manually to have a proper thresholding value for consistent outcomes. For example, as shown in Fig. 4(b), the contours of M_1 and T_1 components of the normal subject well separated.

However, the contour of the MR subject appears like only having a single component (Fig. 6(b)).

Furthermore, by setting c_{con} manually, the thresholding contours of M_1 and T_1 components at

overlapping conditions were obtained (Fig. 4(c) and Fig. 6(c)). Fig. 6(e) shows that the contour of S_2 (the MR subject) looks like just having a single component and occurs other contour after the event of S_2 contour. In the same way, to identify the components of S_2 , the thresholding contour of A_2 and P_2 components at overlapping condition were obtained (Fig. 6(f)). The TR subject seemed only single dominant of S_2 contour (Fig. 7(e)). However, after the magnitude thresholding operation, the thresholding contours of the A_2 and P_2 components at overlapping condition were obtained (Fig. 7(f)). Moreover, although setting its thresholding operation has been performed (e.g. Fig. 5(e)), the contours of the S_2 components often were not visible (e.g. Fig. 5(f)). Also for identification of the contours of S_1 components. The magnitude thresholding method may be less accurate when the A_2 and P_2 components or the M_1 and T_1 components have very short duration (i.e., when they look like a single contour).

Additionally, if both the thresholding contours at overlapping condition, e.g. Figs. 4(c) and 4(f), localization of the split time S_1 and S_2 components became difficult. It is affected by the heart valve closure of the left side (M_1 and A_2) almost simultaneously with the right side (T_1 and P_2). Therefore, t_{COG} of each the thresholding contour should be performed to specify the split time of the S_1 and S_2 components. However, if the contours of the S_1 and S_2 components, respectively, appeared as a single contour component, determination of the correct split time would be impossible.

We found in our experimental results that S_2 had shorter t_{dur} than S_1 for the three groups of subjects. Its t_{dur} caused by closing rapidly of semilunar valves (A_2 and P_2) and vibrating of the fluid of blood that surrounds the valves in a shorter interval [7], [24]. Additionally, the t_{dur} average percentage of S_2 is shorter than the t_{dur} average

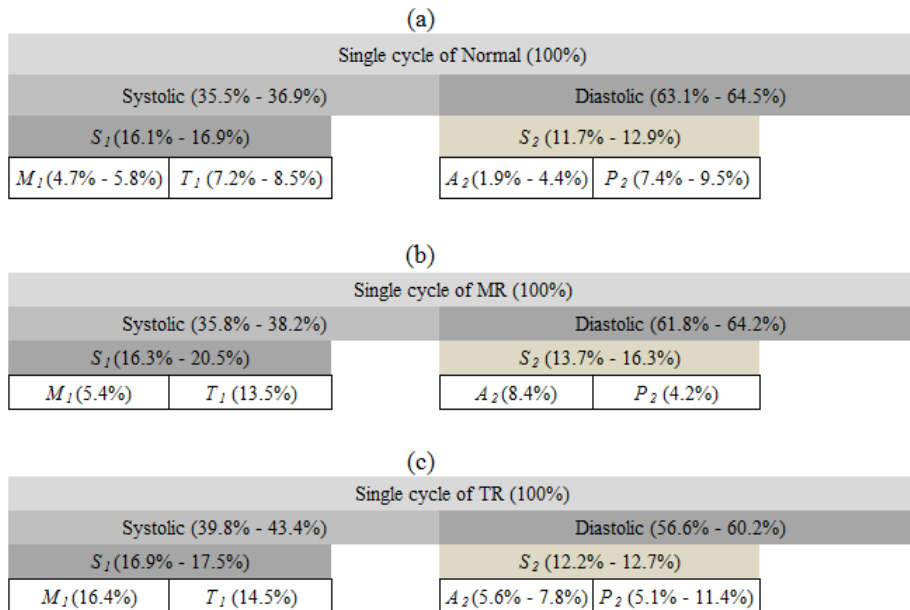
percentage of S_1 towards the t_{dur} average percentage of single cycle for the three groups of subjects (Figs. 8). The result of Table I for the normal subject was similar to Luisada et al. [8]. Their experimental results that the average t_{dur} of S_1 was 0.146 s (at the apex) and 0.140 s (at the aortic area) of the subjects with the age above 10 years old, also the average t_{dur} of S_2 in the same conditions was 0.097 s and 0.104 s, respectively.

Earlier studies [13], [15], [16] did not define clearly how to determine the S_1 - S_2 spaced time in their wavelet transform algorithms for the normal subject. In our experimental results, the spaced time (Table I) was slightly different from Debbal and Bereksi-Reguig [13], 0.312 sec., and Vikhe et al. [16], 0.3 sec. In our algorithm, the spaced time was difference between t_{COG} of S_1 and t_{COG} of S_2 in relation to the thresholding contour of S_1 and S_2 , respectively.

Moreover, the spaced time of the MR and TR subjects were longer than the normal subject (Table I). These were caused incompetence of M_1 valve, at the left side of the heart, and T_1 valve, at the right side of the heart, respectively, to close perfectly and resulted in blood backflow from left ventricle to left atrium and from right ventricle to right atrium [11]. Furthermore, for the normal subject, Table I shows that S_2 has higher frequency content than S_1 . The result was similar to [13] and [16]. However, [13] and [16] did not explain obviously how to acquire s_l and s_h of both S_1 and S_2 contour plots. Moreover, frequency content of S_1 is higher than S_2 for MR and TR subjects (Table I).

IV.1. Measurement of the S_1 Components

Splitting of S_1 into its two audible components, M_1 and T_1 , is a normal finding on cardiac auscultation [24].



Figs. 8. Temporal analysis of S_1 and S_2 components relative to the single cycle in percentage (%) of normal (a), MR (b) and TR (c) subjects, respectively.

The normal S_1 split time heard when contraction of the right ventricle is delayed. Such a delay causes delayed T_1 valve closure, thus causing a widening interval between M_1 and T_1 [7]. Therefore, in this study, t_{dur} of T_1 is longer than M_1 for the normal subject as shown in Table I.

The same result also for the MR subject was obtained, except for the TR subject. Furthermore, as shown in Figs. 8 the t_{dur} average percentage of T_1 is longer than the t_{dur} average percentage of M_1 towards the t_{dur} average percentage of single cycle for normal and MR except TR subject. The split time between M_1 and T_1 of the normal subject is similar to data of Stein and Delman [12], i.e. 0.020 to 0.040 s. However, the result was different from Debbal and Bereksi-Reguig [13], 0.005 s. Debbal and Bereksi-Reguig [13] did not explain systematically and clearly of their split time measurement. The fact that the S_1 split time may be helpful in certain disease states [24]. In our study, the S_1 split time for pathological subjects was longer than the normal subject. This is due to the heart sounds of a split lengthwise (heavier) [11]. However, M_1 and T_1 are occasionally perceived as a single sound, called S_1 . Most times, only S_1 is heard because M_1 and T_1 are separated by less than 0.020 s [7]. The absence of S_1 split was shown of our experimental data. Additionally, the M_1 valve and myocardial surrounding of its valve, at the left side of the heart, are larger and thicker than the T_1 valve and its supporting cardiac muscles, at the right side of the heart.

The left side develops a higher pressure than the right side. Thus, rate of myocardial contraction of the left side is higher and turbulent velocity of blood flow more rapidly to close M_1 valve [7], [11]. These events cause the frequency content of M_1 is higher than T_1 (e.g. Fig. 4(b)). The similar results are shown in Table I, for the three groups of subjects.

IV.2. Measurement of the S_2 Components

In order to be differentiated and heard as two distinct sounds, the A_2 closure sound and the P_2 closure sound must be separated by more than 0.020 s [6]. A presence of S_2 split time is caused by a small time delay between the aortic component and the pulmonic component. Closing of A_2 and P_2 valves coincides with the termination of left ventricular ejection and right ventricular ejection, respectively. Normally, the closing P_2 valve occurs after the closing A_2 valve.

Since right ventricular ejection terminates after left ventricular ejection [25]. Thus, in our experimental results, t_{dur} of P_2 is longer than A_2 of the normal and TR (Table I), except for the MR subject. This was cause of systolic murmur of the pathological subject (MR). Additionally, as shown in Figs. 8 the t_{dur} average percentage of P_2 is longer than the t_{dur} average percentage of A_2 towards the t_{dur} average percentage of single cycle for the normal and TR except the MR subject. The A_2 - P_2 split for two conditions of the normal subject (Table I) was similar to [25]. However, the result was different from Debbal and Bereksi-Reguig [13],

[15], 0.006 s and Vikhe et al. [16], 0.009 s. Because earlier studies [13], [15], [16] did not explain systematically of their split time measurement. The time delay between A_2 and P_2 is highly crucial clinically to specify the presence and degree of respiratory splitting and the relative intensities of A_2 and P_2 [25]. Nevertheless, S_2 normal split may as well be absent if the A_2 sound masks the P_2 sound or conversely [3]. It was revealed of our experimental data (e.g. Fig. 5(e)). Thus, the S_2 frequently emerges as a single component [26]. Additionally, when the left ventricle relaxes, its pressure falls more rapidly (below the pressure in the aorta) than the right ventricle (below the pressure in the pulmonary artery). These occurrences cause rate of a slightly backflow of blood and recoiling of the elastic fibres in the wall of the aorta are higher to close the A_2 valve. The vibrations associated with these events produce the S_2 sound, which the A_2 closure sound is heard louder than the P_2 closure sound [7], [11], [27]. Thus, the frequency content of A_2 is higher than P_2 (e.g. Fig. 4(e)). The similar results are shown in Table I for the three groups of subjects.

Earlier studies [13], [15], [16] did not clearly explain how to measure the A_2 - P_2 split using wavelet coefficients. Moreover, their experimental results concerning two contours of A_2 and P_2 , only presented at adjacent condition in time. However, in our experimental results, both contours could also be appeared as a single component (such as Fig. 5(d)) and overlapping (such as Fig. 4(d)) conditions. The split time was calculated based on the difference between t_{COG} of A_2 and t_{COG} of P_2 from the thresholded contours of A_2 and P_2 , respectively.

The similar results were shown in our previous research, about cardiac valvular hemodynamic point of view [28]. Most of the split time results were similar to data of Felner [25], 0.02 to 0.08 s. A simultaneous decrease in blood flow toward the left side of the heart results in a shorter left ventricular ejection time [7].

Thus, closing pressure of A_2 valve slightly ahead of P_2 valve, contributes to the S_2 split time.

IV.3. Impact of the Heart Sound Characterization for Modelling and Study in Medicine

The heart sound is indicated by fast changes and transients in frequency as the time associated with intracardiac valvular events. The closure of M_1 and T_1 valves (S_1 components) also A_2 and P_2 valves (S_2 components) show dominant frequency phenomenon in the central stage of the three stages of the generation of S_1 and S_2 , respectively [8], [9]. In our experimental results, as shown in Table II, from the contour of two dimensional representations for the three groups of subjects, the average time position as well as the percentage of occurrence of the early valve closure, the magnitude achieves a peak, and the ending valve closure of each S_1 and S_2 components relative to the cardiac cycle associated with each their frequency content gave more simply and easily seen.

TABLE II
POSITION OF S_1 AND S_2 COMPONENTS AND EACH THEIR FREQUENCY CONTENT RELATIVE TO THE SINGLE CYCLE OF THE NORMAL,
THE MR, AND THE TR SUBJECTS, RESPECTIVELY

S_1 components		Closing M_1 valve (left side of the heart)			Closing T_1 valve (right side of the heart)		
Magnitude of contour		<i>early</i>	<i>peak</i>	<i>end</i>	<i>early</i>	<i>peak</i>	<i>end</i>
Normal	average time position (s)	0.013-0.018	0.030-0.038	0.050-0.063	0.035-0.043	0.068-0.072	0.099-0.100
	position of single cycle (%)	1.7-2.4	3.8-5.1	6.4-8.4	4.5-5.7	8.7-9.6	12.8-13.2
	average freq. content (in scale)	0.017-0.020	0.013-0.024	0.017-0.020	0.024-0.025	0.018-0.031	0.024-0.025
MR	average time position (s)	0.010	0.031	0.056	0.068	0.128	0.183
	position of single cycle (%)	1.2	3.6	6.5	7.9	14.9	21.3
	average freq. content (in scale)	0.034	0.028-0.042	0.034	0.055	0.044-0.066	0.055
TR	average time position (s)	0.011	0.068	0.145	0.050	0.105	0.168
	position of single cycle (%)	1.3	8.7	18.5	6.4	13.4	21.5
	average freq. content (in scale)	0.034	0.023-0.043	0.034	0.060	0.053-0.067	0.060
S_2 components		Closing A_2 valve (left side of the heart)			Closing P_2 valve (right side of the heart)		
Magnitude of contour		<i>early</i>	<i>peak</i>	<i>end</i>	<i>early</i>	<i>peak</i>	<i>end</i>
Normal	average time position (s)	0.282-0.288	0.293-0.296	0.301-0.317	0.292-0.312	0.330-0.345	0.364-0.380
	position of single cycle (%)	36.8-37.7	37.5-39.5	38.5-42.3	39.0-39.9	44.1	47.2-48.6
	average freq. content (in scale)	0.016-0.017	0.012-0.020	0.016-0.017	0.026-0.029	0.020-0.033	0.026-0.029
MR	average time position (s)	0.317	0.350	0.391	0.379	0.398	0.418
	position of single cycle (%)	36.5	40.2	45.0	43.7	45.8	48.1
	average freq. content (in scale)	0.034	0.023-0.042	0.034	0.037	0.032-0.040	0.037
TR	average time position (s)	0.314-0.327	0.340-0.344	0.368-0.376	0.320-0.334	0.339-0.375	0.361-0.419
	position of single cycle (%)	40.1-43.9	43.4-46.2	48.0-49.4	41.0-44.8	43.3-50.3	46.1-56.3
	average freq. content (in scale)	0.023-0.033	0.017-0.041	0.023-0.033	0.043-0.067	0.035-0.074	0.043-0.067

For the early valve closure of each S_1 and S_2 components, the contour has narrow frequency content with the ascending magnitude. Furthermore, the magnitude achieves a peak with the fairly wide frequency content. Moreover, the magnitude gradually falls and most of the frequency contents slowly narrowed at the ending valve closure. Most of the early closure of the T_1 valve is simultaneous with the M_1 magnitude peak event for the normal subject. However, for the MR and TR, time delay between early closure of the T_1 valve and the M_1 magnitude peak was occurred. Additionally, most of the early closure of the P_2 valve is simultaneous with the A_2 magnitude peak occurrence for the normal subject.

However, time delay between early closure of the P_2 valve and the A_2 magnitude peak of the MR and TR was ensued.

In previous researches, the basic models of the analysis and synthesis of S_1 and S_2 have been performed. Chen et al. [29] have been developed the exponentially damped sinusoid model of S_1 . However, their research only involved the mitral valve in valvular component. Additionally, the matching pursuit method presented a sum of Gaussian sinusoids located with high resolution in the time-frequency plane [6]. However, the study did not yet address each component of S_1 and S_2 , respectively.

Furthermore, Xu et al. [26], [30] have been modelled A_2 and P_2 components through narrow-band nonlinear transient mono-component chirp signals of short duration with energy distribution concentrated along their instantaneous frequency. However, they proposed method had limitation when the splitting interval in very short duration (< 20 ms) and appear as mono-component signal in the time-frequency map.

In our study, the splitting interval could be easily obtained by using the COG of each the component contour. Meanwhile, in our proposed method, the characterization of duration percentage of S_1 and S_2

components relative to the single cycle (Figs. 8) could be better described variations of the closing duration of the heart valves. Additionally, the percentage of the average time position of the early valve closure, the magnitude reaches a peak, and the ending valve closure of each S_1 and S_2 components relative to the cardiac cycle associated with each their frequency content of a contour in the time-scale domain, more ease understanding visually (Table II).

Thus, the comprehensive model of S_1 and S_2 that more represented the components of the heart sound can be easily obtained. Therefore, the characterization was considered very helpful in development of the heart sound modelling.

In the study of auscultation technique, Horiszny [31] has developed a program to teach cardiac auscultation skills for 18 family practice residents through a Cardionics CardioSim Digital Heart Sound Simulator® (Cardionics, Inc., Houston). He was only limited in teaching auditory and carried on a simulator and not patients. Meanwhile, in our study, the physiologic splitting of S_2 could be explained more easily realized both visually (e.g. Figs. 4) and in the form of temporal-scale parameters.

Thus, our proposed method was expected valuable to assist in the study of auscultation technique from the signal processing method point of view. Application of our proposed method was adequate to characterize objectively, clearly, systematically, and comprehensively in capturing temporal and frequency-related parameters of the heart sound signals.

The duration of the diastole is longer than the systole in each cardiac cycle. During systole, the duration of T_1 valve closure is longer and occurs after M_1 valve closure (except for TR subject). In diastole, the duration of P_2 valve closure is longer and ensues after A_2 valve closure (except for MR subject). The mechanical activities of the left side of the heart (M_1 and A_2) need more force to close

their valves, while the frequency content of M_1 and A_2 are higher than mechanical activities of the right side (T_1 and P_2).

Our method could overcome difficulties of traditional auscultation and could distinguish between normal and pathologic systolic murmur (MR and TR) subjects. Interpretation of our experimental study could not be generalized to all cases of normal, MR, and TR subject, respectively.

It was caused limitation of experimental data, measurement condition, and individual variation. Additionally, the method did not work, if the contours of the S_1 and S_2 components, respectively, appeared as a single component. However, we believed that the characterization provided very valuable and important information for clinical diagnosing and for understanding about mechanisms of cardiac valves functions.

Moreover, the characterization contributes on developing of heart sound modelling and study about auscultation technique of medical students for educational purpose. For further research, classification of both normal and pathological heart sounds based on their essential characteristics is important for cardiac diagnosis.

V. Conclusion

Characterization of the heart sounds using signal processing and extensive characterization based on wavelet analysis has shown ability to overcome difficulties of traditional auscultation. Furthermore, the method was more capable in capturing temporal and frequency-related parameters while compared with the previous research, such as FFT and STFT methods.

The characteristics of each pattern of the heart sounds can be extracted more precisely by using a flexible window modulation.

The magnitude thresholding operation and COG of the wavelet contour were performed adequately to restrict temporal and frequency-related evidence of valvular activities. Hence, our proposed method is very useful for diagnosis and for gaining our understanding about mechanisms of cardiac valves functions. Moreover, the important characteristics in the form temporal and frequency-related parameters would be impact on development of heart sound modelling and study of auscultation technique for medical students. We believed that all these important characteristics could be used for detection of healthy subject as well as certain disease states.

Thus, the application of our method was considered valuable to explain mechanisms of cardiac valves functions. We expected that the method would be helpful for clinical diagnosis as well as very useful for developing of heart sound modelling and for educational purpose of medical students in auscultation technique.

Next topic of our research was addressed for classification of heart sounds based on their essential characteristics.

Acknowledgements

This study was supported by Directorate General of Higher Education, Ministry of National Education of Indonesia under Graduate Education Scholarship and Sandwich Program. The authors would like to thank Somali, MD for his assistance and permission to collect data at Kebonjati Hospital, Bandung.

References

- [1] Z. Jiang, S. Choi, A Cardiac Sound Characteristic Waveform Method for In-Home Heart Disorder Monitoring with Electric Stethoscope, *Expert Systems with Applications*, vol. 31, 2006, pp. 286 - 298.
- [2] S. Sun, H. Wang, Z. Jiang, Y. Fang, T. Tao, Segmentation-Based Heart Sound Feature Extraction Combined with Classifier Models for A VSD Diagnosis System, *Expert Systems with Applications*, vol. 41, Issue 4, Part 2, March 2014, pp. 1769 - 1780, ISSN 0957-4174.
- [3] Sumathi, R., Kirubakaran, E., Krishnamoorthy, R., Multi class multi label based Fuzzy associative classifier with genetic rule selection for coronary heart disease risk level prediction, (2014) *International Review on Computers and Software (IRECOS)*, 9 (3), pp. 533-540.
- [4] Nalini, D., Periasamy, R., Lloyd and minkowski based K-means clustering for effective diagnosis of heart disease and stroke, (2015) *International Review on Computers and Software (IRECOS)*, 10 (6), pp. 573-579.
- [5] Gurram, D., Narasinga Rao, M.R., A decision support system for predicting heart disease using multilayer perceptron and factor analysis, (2015) *International Review on Computers and Software (IRECOS)*, 10 (8), pp. 799-804.
- [6] X. Zhang, L.G. Durand, L. Senhadji, H.C. Lee, J.L. Coatrieux, Analysis-Synthesis of the Phonocardiogram Based on the Matching Pursuit Method, *IEEE Transactions on Biomedical Engineering*, vol. 45 n. 8, August 1998, pp. 962 - 971.
- [7] D. Labus, B.H. Mayer, J. Munden, L. Schaeffer, G. Thompson (eds.), *Heart Sounds Made Incredibly Easy* (Lippincott Williams & Wilkins, 2005).
- [8] A.A. Luisada, F. Mendoza, M.M. Alimurung, The Duration of Normal Heart Sounds, *British Heart Journal*, vol. 11 n. 1, 1949, pp. 41 - 47.
- [9] A.A. Luisada, M.D., C.K. Liu, M.D., C. Aravanis, M.D., M. Testelli, M.D., J. Morris, B.A., Chicago, Ill., On The Mechanism of Production of the Heart Sounds, *American Heart Journal*, vol. 55, March 1958, pp. 383 - 399.
- [10] Z. Syed, D. Leeds, D. Curtis, F. Nesta, R.A. Levine, J. Guttg, A Framework for The Analysis of Acoustical Cardiac Signals, *IEEE Transactions on Biomedical Engineering*, vol. 54 n. 4, April 2007, pp. 651 - 662.
- [11] B. Erickson, *Heart Sounds and Murmurs across the Lifespan* (4th ed., EGC, Jakarta, Indonesian Version, 2007).
- [12] E. Stein, A.J. Delman, *Rapid Interpretation of Heart Sounds and Murmurs* (2nd ed., EGC, Jakarta, Indonesian Version, 1994).
- [13] S.M. Debbal, F. Bereksi-Reguig, Wavelet Transform Analysis of the Normal Cardiac Sounds, *Biomedical Soft Computing and Human Sciences*, vol. 12 n. 1, 2007, pp. 53 - 58.
- [14] J.J. Lee, S.M. Lee, I.Y. Kim, H.K. Min, S.H. Hong, Comparison between short time Fourier and wavelet transform for feature extraction of heart sound, *Proceedings of the IEEE Region 10 Conference, TENCON 99*, vol. 2, December 1999, pp. 1547 - 1550.
- [15] S.M. Debbal, F. Bereksi-Reguig, Automatic Measure of the Split in the Second Cardiac Sound by Using the Wavelet Transform Technique, *Computers in Biology and Medicine*, vol. 37, 2007, pp. 269 - 276.
- [16] P.S. Vikhe, S.T. Hamde, N.S. Nehe, Wavelet transform based abnormality analysis of heart sound, *Proceedings of International Conference on Advances in Computing, Control, and Telecommunication Technologies*, December 28-29, 2009,

- pp. 367 - 371.
- [17] Z. Tu, G. Cao, Q. Li, X. Zhang, J. Shi, Improved methods for detecting main components of heart sounds, *IEEE International Conference on Natural Computation (ICNC)*, vol. 7, August 10-12, 2010, pp. 3585-3588.
- [18] L.T. Hall, J.L. Maple, J. Agzarian, D. Abbott, Sensor System for Heart Sound Biomonitor, *Microelectronics Journal*, vol. 31, 2000, pp. 583 - 592.
- [19] H. Liang, S. Lukkariinen, I. Hartimo, Heart Sound Segmentation Algorithm Based on Heart Sound Envelopogram, *Computers in Cardiology*, vol. 24, 1997, pp. 105 - 108.
- [20] M.S. Obaidat, Phonocardiogram Signal Analysis: Techniques and Performance Comparison, *Journal of Medical Engineering & Technology*, vol. 17 n. 6, November/December 1993, pp. 221 - 227.
- [21] R. Polikar, *The Wavelet Tutorial Part III Multiresolution Analysis and the Continuous Wavelet Transform* (2nd ed., June 5, 1996).
- [22] G. Strang, T. Nguyen, *Wavelets and Filter Banks* (Wellesley-Cambridge Press, 1997).
- [23] B. Ergen, Y. Tatar, H.O. Gulcur, Time-Frequency Analysis of Phonocardiogram Signals Using Wavelet Transform: A Comparative Study, *Computer Methods in Biomechanics and Biomedical Engineering*, vol. 15 n. 4, 2012, pp. 371 - 381.
- [24] J.M. Felner, The first heart sound, In H.K. Walker, W.D. Hall, J.W. Hurst (Eds.), *Clinical methods: the history, physical, and laboratory examinations* (3rd ed., Butterworth Publishers, Boston, 1990, 117-121).
- [25] J.M. Felner, The second heart sound, In H.K. Walker, W.D. Hall, J.W. Hurst (Eds.), *Clinical methods: the history, physical, and laboratory examinations* (3rd ed., Butterworth Publishers, Boston, 1990, 122-125).
- [26] J. Xu, L.G. Durand, P. Pibarot, Extraction of The Aortic and Pulmonary Components of the Second Heart Sound Using A Nonlinear Transient Chirp Signal Model, *IEEE Transactions on Biomedical Engineering*, vol. 48 n. 3, March 2001, pp. 277 - 283.
- [27] A.G. Tilkian, M.B. Conover, *Understanding Heart Sounds and Murmurs* (Binarupa Aksara, Tangerang, Indonesian Version, 2008).
- [28] R. Hendradi, A. Arifin, M.H. Purnomo, S. Gunawan, Exploration of cardiac valvular hemodynamics by heart sound analysis of hypertensive cardiac disease background patients, *IEEE International Conference on Computational Intelligence and Cybernetics (CyberneticsCom)*, July 12-14, 2012, pp. 153-157.
- [29] D. Chen, L.G. Durand, H.C. Lee, Time-Frequency Analysis of the First Heart Sound. Part 1: Simulation and Analysis, *Medical & Biological Engineering & Computing*, vol. 35, July 1997, pp. 306 - 310.
- [30] J. Xu, L.G. Durand, P. Pibarot, Nonlinear Transient Chirp Signal Modeling of the Aortic and Pulmonary Components of The Second Heart Sound, *IEEE Transactions on Biomedical Engineering*, vol. 47 n. 7, July 2000, pp. 1328 - 1335.
- [31] J.A. Horiszny, M.D., Teaching Cardiac Auscultation Using Simulated Heart Sounds and Small-Group Discussion, *Family Medicine*, vol. 33 n. 1, January 2001, pp. 39 - 44.

Authors' information

¹Graduate Program of Electrical Engineering, Department of Electrical Engineering, Institut Teknologi Sepuluh Nopember Surabaya 60111, Indonesia.

²Graduate Schools of Engineering and Biomedical Engineering, Tohoku University, Sendai 980-8579, Japan.

³Kebonjati Hospital Bandung 40181, Indonesia.

⁴Graduate School of Science and Engineering for Research, University of Toyama 3190 Gofuku, Toyama 930-8555, Japan.

⁵Biomedical Engineering Department, Institut Teknologi Sepuluh Nopember Surabaya 60111, Indonesia.



R. Hendradi received his B.Sc. and M.Sc. degrees in Mathematics Department, University of Gadjah Mada (UGM), Yogyakarta, Indonesia, in 1995 and 2002, respectively. He has been working as an Educational Staff in Mathematics Department, Universitas Airlangga (UNAIR), Surabaya, Indonesia. He is currently pursuing Ph.D. degree at Electrical Engineering Department, Institut Teknologi Sepuluh Nopember (ITS), Surabaya, Indonesia. His present research interests include the biomedical signal processing and particular in time-frequency phonocardiogram analysis. He is a student member of IEEE--Engineering in Medicine and Biology Society (EMBS).



A. Arifin received his B.E. degree in Electronic Engineering from Institut Teknologi Sepuluh Nopember (ITS), Indonesia, in 1996. Since then he has joined Electrical Engineering Department, ITS, as an Educational Staff. He received M.E. and Ph.D. degrees in Electronic Engineering from Tohoku University in 2002 and 2005, respectively, with major in Biomedical Electronic Engineering. Since 2015 he serves as Head of Biomedical Engineering Department, ITS. His research activities are in fields of human movement measurement and analysis, human movement restoration by functional electrical stimulation (FES), biomedical signal and system modelling and analysis, and fuzzy control system. He is a member of IEEE-Engineering in Medicine and Biology Society (EMBS).



H. Shida was born in Sendai, Japan, on February 19, 1987. He received a B.E. degree from Tohoku University, Sendai, Japan in 2008 in Electrical Engineering, and M.E. degrees, also from Tohoku University, in 2012 in Biomedical Engineering. He has been working as a Broadcast Engineer in Broadcast Engineering Department, Japan Broadcasting Corporation (NHK), Tokyo, Japan. His present interests are broadcast engineering to prepare for emergency disaster and development of ultra-high sensitivity camera using HARP image pickup tubes and application examples.



S. Gunawan received his M.D. from Maranatha Christian University, Bandung, Indonesia in 1984. From 1992 to 1994 he was trained as a Clinical Fellow in Cardiology at National Heart Centre, Singapore. From 1985 to 2012 he has been working in Internal Medicine Department at Immanuel Hospital Bandung. He is also a lecturer in the Department of Medicine, Faculty of Medicine, Maranatha Christian University. He is currently a physician at Kebonjati Hospital Bandung.



M. H. Purnomo received his B.E. degree from Institut Teknologi Sepuluh Nopember (ITS), Surabaya, Indonesia in 1985. He received his M.Eng. and Ph.D. degrees from Osaka City University, Osaka, Japan in 1995 and in 1997, respectively. He has joined ITS Surabaya in 1985 and has been a Professor since 2003. His current interests include intelligent system in control biomedical signal and image processing. He is a member of IEEE and International Neural Network Society.



H. Hasegawa was born in Oyama, Japan, in 1973. He received the B.E. degree from Tohoku University, Sendai, Japan in 1996. He received the Ph.D. degree from Tohoku University in 2001. He is presently a Professor at the Graduate School of Science and Engineering for Research, University of Toyama. His main research interest is medical ultrasound, especially diagnosis of cardiovascular system by measurement of its

dynamic properties. Dr. Hasegawa is a member of the IEEE, the Acoustical Society of Japan, the Japan Society of Ultrasonics in Medicine, and the Institute of Electronics, Information and Communication Engineers.



H. Kanai was born in Matsumoto, Japan, on November 29, 1958. He received a B.E. degree from Tohoku University, Sendai, Japan in 1981, and M.E. and the Ph. D. degrees, also from Tohoku University, in 1983 and in 1986, both in Electrical Engineering. From 1986 to 1988 he was with the Education Centre for Information Processing, Tohoku University, as a research associate. From 1990 to 1992 he was a lecturer in the Department of Electrical Engineering, Faculty of Engineering, Tohoku University. From 1992 to 2001 he was an associate professor in the Department of Electrical Engineering, Faculty of Engineering, Tohoku University. Since 2001 he has been a professor in the Department of Electronic Engineering, Graduate School of Engineering, Tohoku University. Since 2008 he has been also a professor in the Department of Biomedical Engineering, Graduate School of Biomedical Engineering, Tohoku University. From 2012 to 2015 he was a dean of Graduate School of Engineering, Tohoku University. From 2015 he has been a vice president (for Research Consolidation and University Reform), Tohoku University. His present interests are in transcutaneous measurement of the heart wall vibrations and myocardial response to propagation of electrical potential and cross-sectional imaging of elasticity around atherosclerotic plaque with transcutaneous ultrasound for tissue characterization of the arterial wall. Dr. Kanai is a member of the Acoustical Society of Japan, a fellow of the Institute of Electronics Information and Communication Engineering of Japan, a member of the Japan Society of Ultrasonics in Medicine, Japan Society of Medical Electronics and Biological Engineering, and the Japanese Circulation Society. Since 1998, he has been a member of Technical Program Committee of the IEEE Ultrasonic Symposium. Since 2008, he has been an International Advisory Board of International Acoustical Imaging Symposium. Since 2011, he has been a Board Member of International Congress on Ultrasonics. Since 2012, he has been an editor of Journal of Medical Ultrasonics and Japanese Journal of Medical Ultrasonics. Since 2013, he has been an associate editor of the IEEE Transaction on UFFC.